Is low frequency ocean sound increasing globally?

Jennifer L. Miksis-Olds and Stephen M. Nichols

Citation: The Journal of the Acoustical Society of America **139**, 501 (2016); doi: 10.1121/1.4938237
View online: https://doi.org/10.1121/1.4938237
View Table of Contents: https://asa.scitation.org/toc/jas/139/1
Published by the Acoustical Society of America

Is low frequency ocean sound increasing globally?

Jennifer L. Miksis-Olds[a] and Stephen M. Nichols
Applied Research Laboratory, The Pennsylvania State University, State College, Pennsylvania 16804, USA

(Received 15 April 2015; revised 16 November 2015; accepted 7 December 2015; published online 22 January 2016)

Low frequency sound has increased in the Northeast Pacific Ocean over the past 60 yr [Ross (1993) Acoust. Bull. **18**, 5–8; (2005) IEEE J. Ocean. Eng. **30**, 257–261; Andrew, Howe, Mercer, and Dzieciuch (2002) J. Acoust. Soc. Am. **129**, 642–651; McDonald, Hildebrand, and Wiggins (2006) J. Acoust. Soc. Am. **120**, 711–717; Chapman and Price (2011) J. Acoust. Soc. Am. **129**, EL161–EL165] and in the Indian Ocean over the past decade, [Miksis-Olds, Bradley, and Niu (2013) J. Acoust. Soc. Am. **134**, 3464–3475]. More recently, Andrew, Howe, and Mercer's [(2011) J. Acoust. Soc. Am. **129**, 642–651] observations in the Northeast Pacific show a level or slightly decreasing trend in low frequency noise. It remains unclear what the low frequency trends are in other regions of the world. In this work, data from the Comprehensive Nuclear-Test Ban Treaty Organization International Monitoring System was used to examine the rate and magnitude of change in low frequency sound (5–115 Hz) over the past decade in the South Atlantic and Equatorial Pacific Oceans. The dominant source observed in the South Atlantic was seismic air gun signals, while shipping and biologic sources contributed more to the acoustic environment at the Equatorial Pacific location. Sound levels over the past 5–6 yr in the Equatorial Pacific have decreased. Decreases were also observed in the ambient sound floor in the South Atlantic Ocean. Based on these observations, it does not appear that low frequency sound levels are increasing globally.
 [http://dx.doi.org/10.1121/1.4938237]

[WWA] Pages: 501–511

I. INTRODUCTION

Low frequency (10–100 Hz), deep water ambient sound levels in the Northeast Pacific Ocean have increased at approximately 3 dB/decade (0.55 dB/yr) up until the 1980s (Ross, 1993, 2005; Andrew *et al.*, 2002; McDonald *et al.*, 2006) and then slowed to 0.2 dB/yr (Chapman and Price, 2011). Most recent measurements in this region show a leveling or slight decrease in the sound levels since the late 1990s despite increases in the number and size of ships (Andrew *et al.*, 2011). In the Indian Ocean at Diego Garcia, the low frequency (5–115 Hz) ocean sound floor has increased 2–3 dB over the past decade (Miksis-Olds *et al.*, 2013, 2014). It remains unclear what the low frequency long-term or short-term trends are in other regions of the world. The observed increasing trends in both the Pacific and Indian Oceans have been attributed, in part, to increases in noise produced by shipping (Andrew *et al.*, 2002; McDonald *et al.*, 2006; McKenna *et al.*, 2012; Frisk, 2012; Miksis-Olds *et al.*, 2013), yet decreases of sound levels in the Northeast Pacific were observed as shipping activity continued to rise (Andrew *et al.*, 2011; Wilcox *et al.*, 2014) Recent observations of the prevalence of seismic airgun activity in the Atlantic Ocean has increased the awareness of this source type and its increasing contribution to the ocean soundscape (Klinck *et al.*, 2012; Nieurkirk *et al.*, 2012).

As the effects of climate change continue to be recognized and understood, the noise produced from changing ice dynamics, and other yet to be identified changes in natural source mechanisms, should also be considered in relation to observed ocean sound trends. Low frequency noise produced from ice has already been identified as a large contributor to local soundscapes and detected at basin-scale ranges (Gavrilov *et al.*, 2008; Matsumoto *et al.*, 2014), and this component of the soundscape will continue to change as polar dynamics change. Global climate change is projected to impact the frequency, intensity, timing, and distribution of hurricanes and tropical storms (Michener *et al.*, 1997), which will affect ocean soundscapes at local, regional, and basin scales. The extent to which climate change will impact the acoustic ecology of vocalizing whales, and hence the resulting regional soundscapes, is not yet certain. However, a gradual decrease in the acoustic frequency of blue and pygmy blue whale vocalizations over time has been observed, and many hypotheses on the cause for the decline have been presented, including indirect impacts of climate change (McDonald *et al.*, 2009; Gavrilov *et al.*, 2012).

This study examined decadal trends in ambient sound levels in the South Atlantic and Equatorial Pacific Oceans for comparison to the trends identified in the Northeast Pacific and Indian Oceans (Ross, 1993, 2005; Andrew *et al.*, 2002; McDonald *et al.*, 2006; Chapman and Price, 2011; Miksis-Olds *et al.*, 2013, 2014). Data from the Comprehensive Nuclear-Test Ban Treaty Organization International Monitoring System (CTBTO IMS) were analyzed from recording locations off Ascension Island (South Atlantic) and Wake Island (Equatorial Pacific). Neither of these locations is located in near proximity to any major shipping lanes. Spectrum levels were analyzed

[a]Electronic mail: jlm91@arl.psu.edu

over the full spectrum (5–115 Hz) of the recordings as well as in three 20-Hz bands and reported in percentile values to be consistent with the methods established in Miksis-Olds *et al.* (2013) for the Indian Ocean. Regression and time series analysis were conducted on each percentile to fully characterize the acoustic patterns beyond the average conditions. Frequency correlation matrices are used to provide insight into changing source characteristics by comparing data from the first and last years in each data set.

II. METHODS

A. Acoustic recordings

Recordings from the CTBTO IMS hydrophone triads deployed on opposite sides of Wake Island (H11) in the Equatorial Pacific, Ascension Island (H10) in the South Atlantic Ocean, and Diego Garcia (H08) in the Indian Ocean were made available by the AFTAC/US NDC (Air Force Tactical Applications Center/U.S. National Data Center) (Fig. 1). The sensors are positioned in the deep sound channel at a depth of 600–1400 m, depending on location. The island and surrounding bathymetry interfere with the deep sound channel, effectively blocking sound propagation (Pulli and Upton, 2001). This results in different acoustic "views" from each side of the island and provides the opportunity to examine the dynamics of regional soundscapes and their contributing sources as a function of north−south direction.

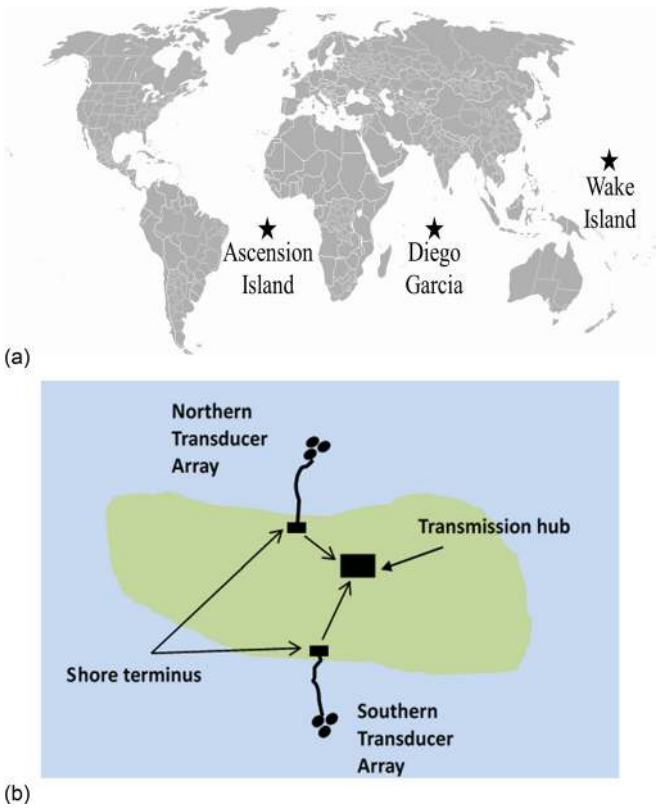

FIG. 1. (Color online) (A) Hydrophone locations at CTBTO stations: H08 Diego Garcia, H10 Ascension Island, and H11 Wake Island. (B) General CTBTO IMS location schematic. Hydrophones triads on each side of the islands were spaced approximately 2 km apart.

Data were sampled continuously at a 250 Hz sampling rate and 24 bit A/D resolution. The hydrophones were calibrated individually prior to initial deployment in January 2002 and re-calibrated while at-sea in 2011. All hydrophones had a flat (3 dB) frequency response from 8 to 100 Hz. Information from individual hydrophone response curves was applied to the data to obtain absolute values over the full frequency spectrum (5–115 Hz). Data less than 5 Hz and from 115 to 125 Hz were not used due to the steep frequency response roll-off at these frequencies. The range over which sources can be detected varies with signal frequency, location, and noise level. In general, the maximum range individual biological signals could be detected was less than 1000 km across sites with the largest detection areas occurring at the Diego Garcia location (Miksis-Olds *et al.*, 2015).

This study used data recorded from single hydrophones N1 and S1 at each location, except at Diego Garcia where S2 was used instead of S1 due to a shift in calibration. Only one of the triad hydrophones from each side of the island was considered because the close proximity and depths of each hydrophone within a triad was thought to render additional analyses of more than one hydrophone in a triad redundant. The depths of the hydrophones in the deep sound channel at each location were as follows: Ascension N1—847 m, Ascension S1—865 m, Wake N1—731 m, Wake S1—750 m, Diego Garcia N1—1248 m, and Diego Garcia S2—1356 m. Recordings from Wake Island covered over a 5.5 yr time period from 25 April 2007 to 31 December 2012, and recordings from Ascension Island covered an approximate 8 yr period from 4 November 2004 to 31 December 2012. Recordings from Diego Garcia cover a decade from 21 January 2002 to 31 December 2012, and the time series results from this data set were published in Miksis-Olds *et al.* (2013, 2014).

B. Ambient sound measurements

Full spectrum (5–115 Hz) measurements were made and analyzed using spectral levels (dB re $1\mu Pa^2/Hz$). Additionally, spectral level measurements were made in three targeted 20 Hz frequency bands: 10–30 Hz, 40–60 Hz, and 85–105 Hz. The frequency bands were selected to (1) target the dominant frequencies of source types [natural seismic and low frequency baleen whales (10–30 Hz); industry seismic, shipping, and biologics (40–60 Hz); shipping (85–105 Hz)] with the understanding that the full spectrum of any source has the potential to contribute energy to more than one frequency band, and (2) be consistent with the frequency band selection of Miksis-Olds *et al.* (2013) for direct comparison to Indian Ocean observations overlapping the same time periods. Mean spectral levels were calculated using a Hann windowed 15 000 point discrete Fourier transform with no overlap to produce sequential 1-min power spectrum estimates over the duration of the data sets. Averages of the spectral levels in the full spectrum and in each of the three targeted frequency bands were computed using intensity and represent the arithmetic mean of intensity for each minute.

C. Statistical analysis

Five daily percentile parameters (P1, P10, P50, P90, P99) were identified from the 1-min power spectra each day to produce a time series of daily percentile values (Fig. 2). The P50 value is the daily median, and each daily percentile value represents the level below which a certain percent of measurements fall within a single day. A multi-year time series of daily percentile values was used to assess data correlations, trends, and distribution. The time series distributions and bivariate linear correlations among them were examined first. Histograms were plotted for each time series to examine the univariate distributions, and pairwise scatter plots were generated. In order to investigate the long-term trend over multiple years, two methods were explored: (1) linear regression model of sound level by year date was fit for each of the time series, and (2) a nonparametric method using 90-day moving averages was calculated to capture more flexible trends compared to a straight linear regression. A moving window of 90 days was selected because it is approximately a quarterly average reflective of seasonal changes. Values 30 dB greater than the decade average were considered outliers and removed from the analysis, which only impacted the analysis of the P99 time series.

D. Frequency correlation matrices

Annual frequency correlation matrices were constructed to better identify and understand changes in source contributions to the regional soundscapes. To build the correlation matrices from ambient sound recordings, the raw data was first converted into a series of sound spectra using a 10-s FFT, with Hann windowing and 50% window overlap for a 3 min long segment of each hour within a year. This process resulted in sound spectra, in dB re 1 μPa^2/Hz, for each hour in the year of interest, with a 0.1 Hz frequency resolution. The set of spectra can also be seen as a time series of sound level measurements at each frequency. The correlation coefficient was calculated between sound levels at each available pair of frequencies to construct the correlation matrix. A simplified illustration of this procedure is seen in Fig. 3. The correlation coefficient used in this paper is defined as

$$r(f_1,f_2)=\frac{\sum_{i=1}^{n}\left[x(f_1)_i-\overline{x(f_1)}\right]\left[x(f_2)_i-\overline{x(f_2)}\right]}{\sqrt{\sum_{i=1}^{n}\left[x(f_1)_i-\overline{x(f_1)}\right]^2\sum_{i=1}^{n}\left[x(f_2)_i-\overline{x(f_2)}\right]^2}}, \quad (1)$$

where $x(f_1)$ is the set of ambient sound levels, in dB, at frequency f_1. The calculated correlation coefficients form a diagonally symmetric matrix, where the i-by-j element represents the correlation coefficient between noise levels at f_i and f_j. Since the diagonal elements represent the correlation between sound levels at the same frequency, the diagonal

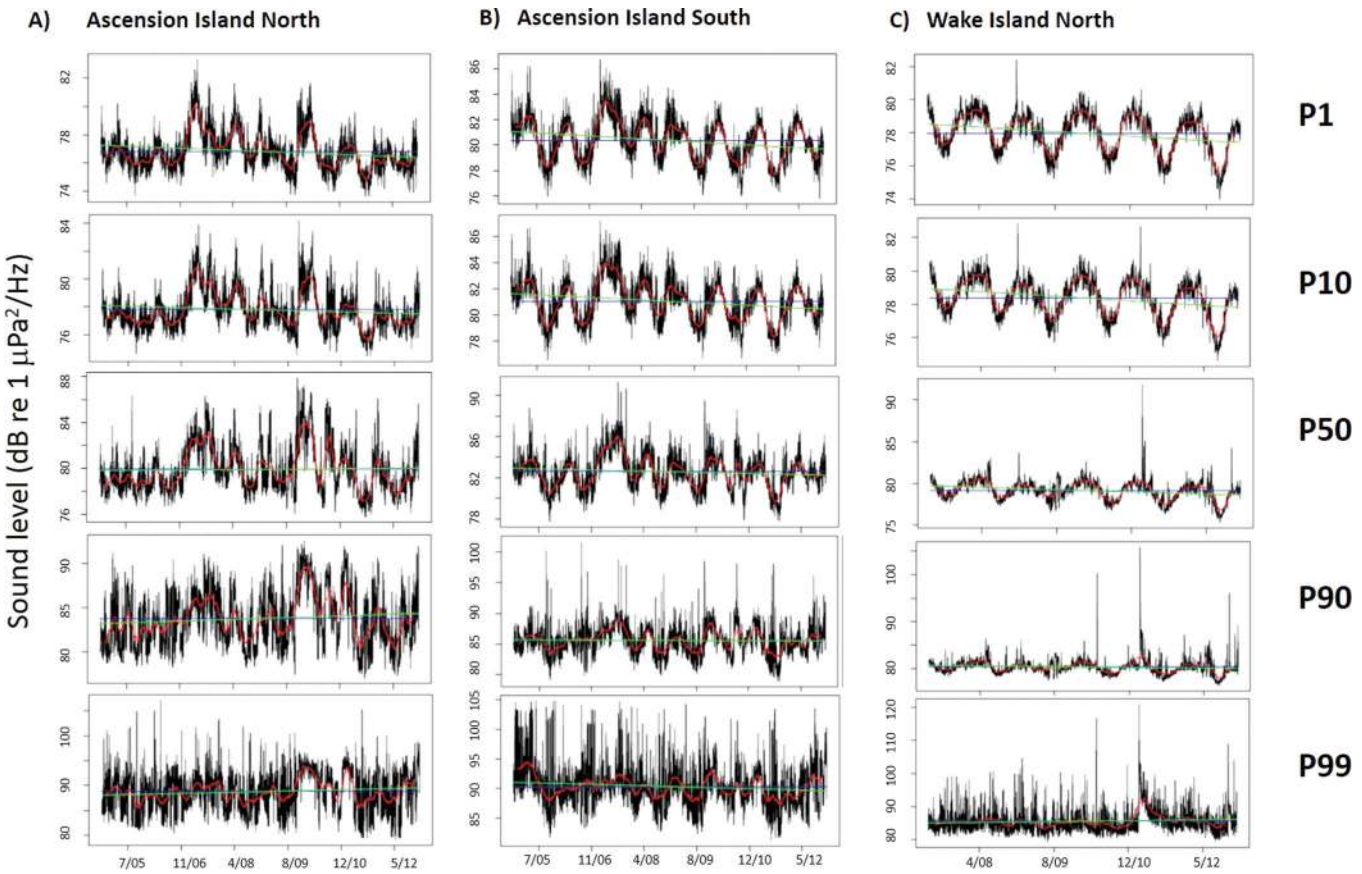

FIG. 2. Full spectrum time series from the (A) Ascension Island North (N1), (B) Ascension Island South (S1), and (C) Wake Island North (N1) locations fitted with moving average (90 days MA) trend (red), linear regression trend (green), and data set average (blue). Linear regression characteristics for all other frequency categories are shown in Table II.

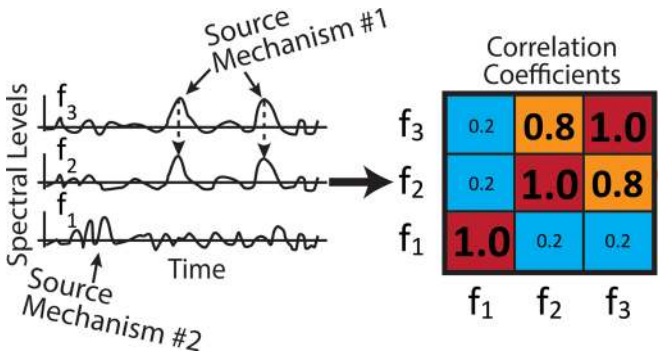

FIG. 3. (Color online) Illustration of the construction of a correlation matrix. The left side depicts the time series of hourly spectral levels at three different frequencies, f_1, f_2, and f_3, all computed from the same time segment of acoustic data. The matrix on the right displays the correlation coefficients between the spectral levels at pairs of frequencies. A color is assigned to each point in the matrix, based on the correlation between the two frequencies, with light colors representing lower correlation and dark colors representing higher correlation. When a source is active in multiple frequency bands, e.g., source mechanism #1, those bands will tend to correlate well with each other; when the primary source in a frequency band is not detected in other bands, e.g., source mechanism #2, that band will not correlate well with the other bands.

elements must always be exactly unity. Figures 4(C) and 4(D) provide examples of such correlation matrices, computed from the spectrograms in Figs. 4(A) and 4(B) and representing the measurements made south of Ascension Island in 2005 and 2012. Going from spectrogram to correlation matrix, the axes are converted from linear to logarithmic scales. High correlation between the sound levels at two frequencies indicates that the corresponding sound levels tend to increase and decrease at the same times, implying that energy in the two frequency bands is due to the same source mechanism. Similarly, large frequency regions in which the sound levels are strongly correlated indicate a frequency range which is due to a particular source. As an example, the 17–28 Hz squares of high correlation in Figs. 4(C) and 4(D) denote a frequency region dominated by biologic sounds, such as those identified by insets (ii) and (iii) of Fig. 4. While the strength of a correlation region does not perfectly relate to the absolute intensity of the source, frequently occurring or higher intensity sounds typically create a stronger correlation than rarely occurring or lower intensity sounds. A notable exception to this tendency would be that if two frequency bands contained continuously high and non-fluctuating levels of sound across the entire time window, the correlation between the two bands would be very low, due to the low variance in sound level.

To compare two different soundscape time periods, the correlation matrices for the two periods were then subtracted from each other, as shown in Fig. 4(E), highlighting frequency regions where the dominant source has changed. The frequency correlation difference matrices presented in this paper represent the differences between the earliest and the latest years available at each location.

III. RESULTS

Daily percentile values were examined to determine the distribution of sound levels for each percentile level, and to determine the correlation between the daily measurements across different percentile levels. The time series of daily percentile sound levels was not Gaussian, and a logarithmic transform did not result in normally distributed data for any of the percentiles at any location. There was little to no correlation between the sound levels in the most extreme percentiles (P1 and P99); correlation values ranged from 0.11 to 0.50 across locations and sites. Strongest correlations (>0.9) were observed between percentiles P1 and P10 and between P90 and P99. The low correlation values between the lowest and highest percentiles comparisons indicated that the trends observed within a single parameter time series (e.g., P1:sound floor) could not be appropriately extrapolated to all other acoustic conditions or parameters (e.g., P50:median or P99:exteme events). Therefore, it was justified and necessary to analyze the multiple sound level parameters and frequency categories separately, as was done previously in the Indian Ocean at CTBTO IMS site Diego Garcia (Miksis-Olds *et al.*, 2013).

Average southern sound levels at Ascension Island ranged from 0 to 4.5 dB higher than concurrent measurements from the north, and the greatest differences were observed for the soundfloor (P1) and P10 percentiles (Table I; Fig. 2). Conversely, sound levels at Wake Island were slightly (0–1.5 dB) higher in the north recordings (Table I). The daily time series analyses showed clear seasonal signals in sound levels recorded at Ascension Island South and Wake Island (Fig. 2). Only Wake Island North is shown in Fig. 2 because the South time series was almost identical. The time series recorded at Ascension Island North showed less of a consistent seasonal signal compared to the other locations.

There was a consistent decreasing linear trend in the ambient soundfloor (P1) and P10 percentiles in both the South Atlantic Ocean at Ascension Island and in the Equatorial Pacific Ocean at Wake Island (Table II). The sign and magnitude of the P50, P90, and P99 trends varied as a function of frequency and location and ranged from a 2.3 dB increase at Ascension Island North to a −3.5 dB decrease projected over a decade at Wake Island North. At Ascension Island, the decreasing trend of the P1 and P10 full bandwidth (5–115 Hz) time series was largely driven by source contributions from the 40–60 Hz band in both the North and South (Table II). The observed increasing trend in the Ascension Island North P90 time series was mainly attributed to the increasing trend seen in the 40–60 Hz and 10–30 Hz bands. In the Ascension Island South recordings, the salient linear trends included a decrease in the P1 and P10 time series (as noted above) and a strong decrease in the P99 time series driven by a decrease in the 85–105 Hz source contribution. Whereas the P90 trend at Ascension Island North showed an overall increase in the full bandwidth, no change was observed in the P90 time series over time in the South (Table II).

The linear trends observed at Wake Island were almost identical in sign and magnitude in the North and South recordings (Table II). As observed at Ascension Island, the ambient sound floor and P10 time series showed a linear decreasing trend at Wake Island, driven mainly by

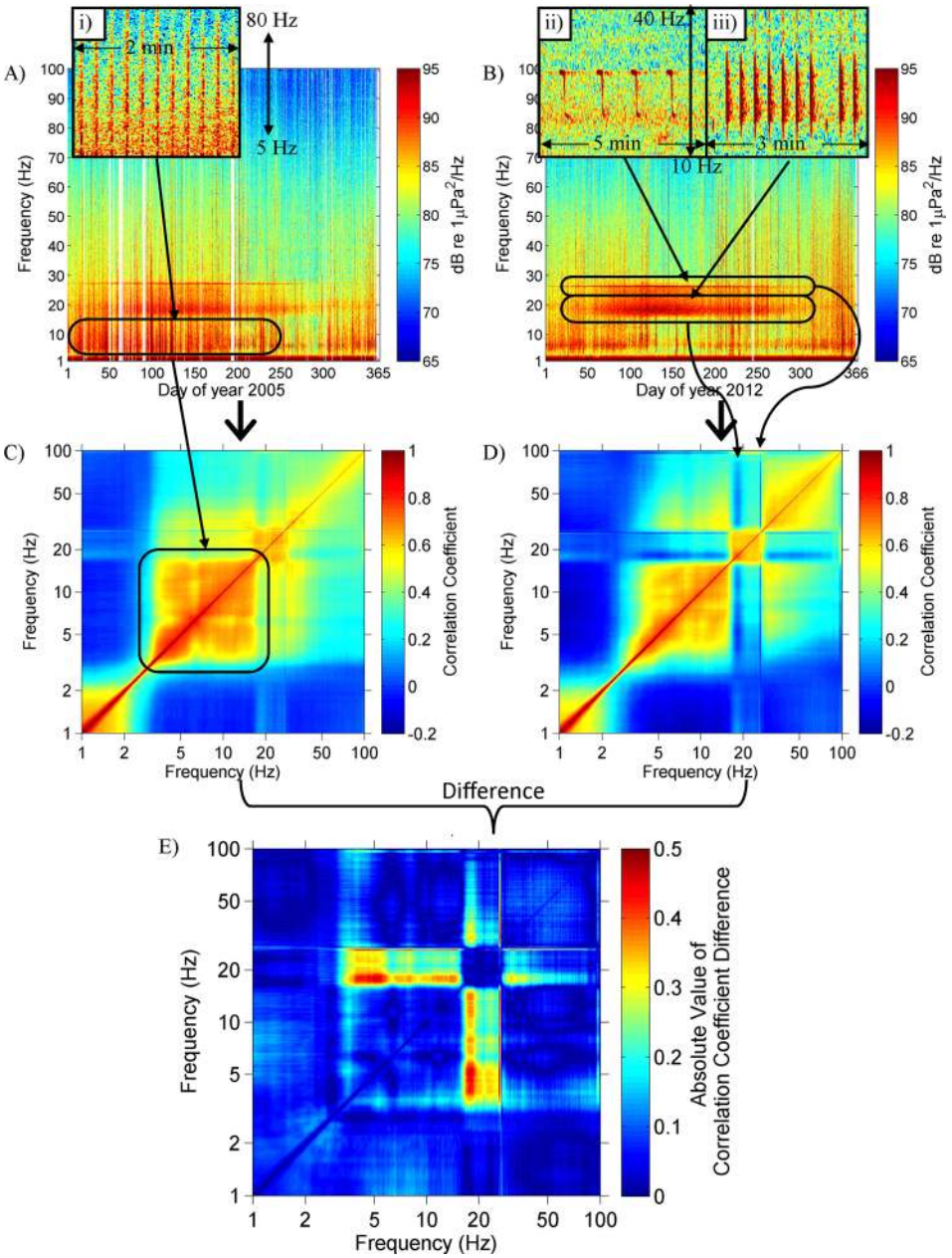

FIG. 4. (Color online) Demonstration of the procedure used to create a frequency correlation difference matrix. Starting with yearly spectrograms from the Ascension Island South (S1) location in 2005 (A) and 2012 (B), the correlation coefficients between spectral levels at different frequencies are computed to form a frequency correlation matrix, with logarithmic axes, for the same location in 2005 (C) and 2012 (D). The frequency correlation matrices are then subtracted from each other to find the correlation difference matrix between the 2 yrs at the same location. Circles highlight specific features discussed in the text.

contributions from the 40 to 60 Hz band. The only increasing trend observed at Wake Island occurred in the P99 time series, and this was attributed solely to an increase in the 10–30 Hz band over the 5.5 yr time period.

The frequency correlation difference matrices found in Fig. 5 highlight changes in the dominant sound sources between the beginning and end of the analysis period. The matrices were constructed from a year of data in the first year (Wake–May 2007–April 2008, Ascension—2005, and Diego Garcia—2003) and 2012 of each data set. Many of the differences identified in the frequency correlation difference matrices are also highlighted in the spectrograms in Figs. 4 and 6, with examples of the characteristic spectrograms of the sources responsible for the changes shown in the insets. The frequency correlation difference matrix in Fig. 5(A) highlights two primary differences in the sound field of Diego Garcia North between 2003 and 2012. First, the region between 5 and 20 Hz shows a substantial change in inter-frequency correlation, produced by the relative absence of seismic airgun signals present in 2012, compared to 2003. Inset (i) of Fig. 6 provides a spectrogram example of the manmade seismic signals encountered frequently during 2003, but not in 2012. Based on the repetition rate of the signal and its broadband frequency spectrum, the signals in the inset were determined to be from seismic airgun sources (Nieukirk *et al.*, 2012). Second, a series of horizontal and vertical lines between 30 and 40 Hz indicated the presence of some multiple frequency tonal signals, which were detected in 2012, but not in 2003. These tonal signals are consistent with pygmy blue whale calls during the austral summer, as circled in Fig. 6(B) (McDonald *et al.*, 2009; Samaran *et al.*, 2010). A typical vocalization detected during that period is seen in inset (ii) of Fig. 6.

TABLE I. Full time series sound level averages and standard deviations for each percentile recorded from the north and south sides of Ascension Island (A) and Wake Island (B). All spectrum levels are reported in dB re 1 μPa^2/Hz. The full time series period at Ascension Island is 8 yr. The full time series duration at Wake Island is 5.5 yr.

(A)					(B)				
		North	South	Difference (dB)			North	South	Difference (dB)
Full 5–115 Hz	P1	76.8 (1.4)	80.4 (1.7)	3.6	Full 5–115 Hz	P1	78.0 (1.2)	76.9 (1.2)	−1.1
	P10	77.8 (1.5)	81.1 (1.7)	3.3		P10	78.4 (1.2)	77.3 (1.2)	−1.1
	P50	79.9 (2.1)	82.6 (1.8)	2.7		P50	79.1 (1.2)	78.2 (1.3)	−0.9
	P90	83.8 (3.2)	85.6 (2.6)	1.8		P90	80.4 (1.8)	79.8 (2.1)	−0.6
	P99	88.8 (4.1)	90.3 (3.8)	1.5		P99	85.6 (4.0)	85.6 (4.1)	0
10–30 Hz	P1	80.2 (1.7)	84.7 (2.0)	4.5	10–30 Hz	P1	79.3 (2.0)	78.3 (1.9)	−1
	P10	81.1 (1.7)	85.3 (1.9)	4.2		P10	79.8 (1.9)	78.9 (1.8)	−0.9
	P50	83.1 (2.3)	86.7 (1.9)	3.6		P50	80.9 (1.8)	80.0 (1.8)	−0.9
	P90	87.0 (3.3)	89.5 (2.7)	2.5		P90	82.4 (2.2)	81.8 (2.5)	−0.6
	P99	92.0 (4.0)	94.0 (3.7)	2		P99	87.4 (3.7)	87.3 (4.0)	−0.1
40−60 Hz	P1	76.2 (1.2)	78.2 (1.3)	2	40–60 Hz	P1	78.9 (1.6)	77.7 (1.5)	−1.2
	P10	77.4 (1.3)	79.1 (1.3)	1.7		P10	79.4 (1.5)	78.2 (1.5)	−1.2
	P50	79.7 (1.8)	80.9 (1.5)	1.2		P50	80.2 (1.5)	79.2 (1.5)	−1
	P90	83.5 (2.8)	84.1 (2.3)	0.6		P90	81.3 (1.6)	80.5 (1.7)	−0.8
	P99	88.2 (4.3)	88.5 (3.8)	0.3		P99	83.0 (2.7)	82.4 (2.7)	−0.6
85–105 Hz	P1	68.7 (1.0)	71.0 (1.3)	2.1	85–105 Hz	P1	73.6 (1.8)	72.5 (1.7)	−1.1
	P10	69.7 (1.1)	71.8 (1.2)	2.1		P10	74.1 (1.7)	73.0 (1.7)	−1.1
	P50	71.7 (1.5)	73.3 (1.4)	1.6		P50	74.8 (1.7)	73.8 (1.6)	−1
	P90	75.1 (2.6)	76.2 (2.3)	1.1		P90	75.8 (1.7)	75.0 (1.7)	−0.8
	P99	80.2 (4.7)	80.6 (3.8)	0.4		P99	77.3 (3.0)	76.6 (2.8)	−0.7

South of Diego Garcia [Fig. 5(B)], the correlation feature present between 2 and 7 Hz was produced by an unknown source mechanism which was present in 2012, but not 2003. Typically, sea−surface wave interactions contribute sound up to 4 Hz, above which, seismic sources (volcanoes, earthquakes, tsunamis, etc.) tend to dominate. This transition usually results in a local minimum sound level around 4 Hz. However, an unidentified sound source introduced a substantial level of sound below 7 Hz for a total of around 100 days. The two periods of time in which this

TABLE II. Linear regression coefficients presented as slope with corresponding estimated sound level change over a decade. The small slope values reflect the daily unit of analysis calculated from approximately 8 and 5.5 yr of data at Ascension Island and Wake Island, respectively. Projected change over a decade (dB) = slope (dB/day)* 365 (days/yr)*10 (yr). Bolded cells indicate no significant change at the 95% significance level.

		Ascension North		Ascension South		Wake North		Wake South	
		Slope (dB/day)	Change (dB)	Slope (dB/day)	Change (dB)	Slope (dB/day)	Change (dB)	Slope (dB/day)	Change (dB)
Full (5–115 Hz)	P1	−0.00029	−1.1	−0.00046	−1.7	−0.00054	−2.0	−0.00053	−1.9
	P10	−0.00020	−0.7	−0.00040	−1.5	−0.00055	−2.0	−0.00056	−2.0
	P50	**0.00006**	**0**	−0.00022	−0.8	−0.00052	−1.9	−0.00055	−2.0
	P90	0.00038	1.4	**−0.00006**	**0**	−0.00030	−1.1	−0.00040	−1.5
	P99	0.00049	1.7	−0.00047	−1.7	0.00056	2.0	0.00031	1.1
10–30 Hz	P1	−0.00009	−0.3	−0.00034	−1.2	−0.00034	−1.2	−0.00034	−1.2
	P10	**0.00001**	**0**	−0.00028	−1.0	−0.00035	−1.3	−0.00037	−1.4
	P50	0.00027	1.0	−0.00010	−0.4	−0.00023	−0.8	−0.00028	−1.0
	P90	0.00055	2.0	**0.00008**	**0**	**0.00003**	**0**	**−0.00012**	**0**
	P99	0.00064	2.3	−0.00027	−1.0	0.00046	1.7	**0.00021**	**0**
40–60 Hz	P1	−0.00049	−1.8	−0.00053	−1.9	−0.00089	−3.2	−0.00088	−3.2
	P10	−0.00039	−1.4	−0.00042	−1.5	−0.00091	−3.3	−0.00090	−3.3
	P50	−0.00009	−0.3	−0.00017	−0.6	−0.00092	−3.4	−0.00094	−3.4
	P90	0.00040	1.5	**0.00009**	**0**	−0.00090	−3.3	−0.00094	−3.4
	P99	0.00073	2.7	**−0.00001**	**0**	−0.00095	−3.5	−0.00085	−3.1
85–105 Hz	P1	−0.00015	−0.5	−0.00021	−0.8	−0.00028	−1.0	−0.00027	−1.0
	P10	−0.00011	−0.4	−0.00013	−0.5	−0.00028	−1.0	−0.00027	−1.0
	P50	**−0.00003**	**0**	**0.00001**	**0**	−0.00026	−0.9	−0.00026	−0.9
	P90	**0.00006**	**0**	**0.00004**	**0**	−0.00021	−0.8	−0.00025	−0.9
	P99	**−0.00016**	**0**	−0.00040	−1.5	−0.00028	−1.0	−0.00026	−0.9

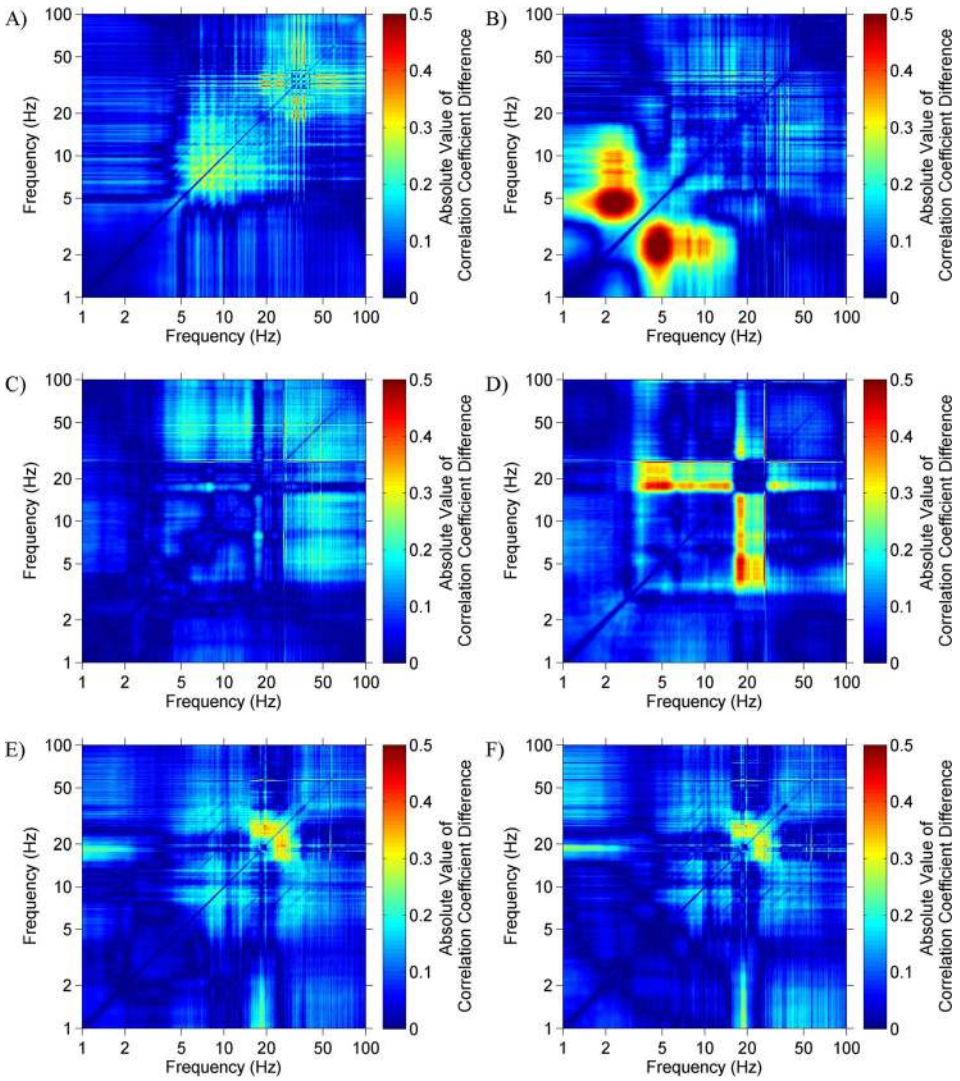

FIG. 5. (Color online) Frequency correlation difference matrices demonstrating the difference in frequency correlation between: 2012 and 2003 for Diego Garcia North (N1) (A) and South (S2) (B), 2012 and 2005 for Ascension Island North (N1) (C) and South (S1) (D), and 2012 and the period from May 2007 to April 2008 for Wake Island North (N1) (E) and South (S1) (F).

source was active are circled in Fig. 6(D). This same source is not present in recordings made on the northern side of Diego Garcia.

On the South of Ascension Island, the large plus-sign shape centered around 20 Hz in Fig. 5(D) [or Fig. 4(E)] reveals a change in the dominant source in the 17–28 Hz range. In 2005, broadband sound from natural and manmade seismic sources contributed significantly to the sound field above 3 Hz, and biologic signals contributed significantly in the 17–28 Hz range. Since both seismic and biologic sources contributed to the 17–28 Hz band, the sound levels in that range correlated moderately well ($r = 0.3$–0.5) with sound levels in the rest of the frequency range dominated by seismic sources, particularly between 3 and 17 Hz. The circle connected to inset (i) in Fig. 4(A) marks the strong presence of seismic sounds in 2005, compared to their relatively reduced presence in 2012. Instead, as seen in Fig. 4(B), the intensity of biologic sounds, produced by Antarctic blue whales [inset (ii)] (Stafford *et al.*, 2004; Samaran *et al.*, 2010) and fin whales [inset (iii)] (Nieukirk *et al.*, 2012), was higher in 2012 than in 2005. As a result of the lower level of seismic airgun signals, and a slight increase in the levels of biologic sounds, the 17–28 Hz band was more due to biologic sources in 2012. Consequently, sound levels in that region were less correlated ($r < 0.2$) with the surrounding broadband region due to seismic sources than in 2005. Since sound levels in the 3–17 Hz and 17–28 Hz bands are less correlated with each other in 2012 than in 2005, the frequency correlation difference matrix seen in Fig. 5(D) shows a region of relatively high change in correlation coefficient at the intersection of the 3–17 and 17–28 Hz bands. This effect was not observed North of Ascension Island. Instead, the lightly shaded patches seen above 30 Hz in Fig. 5(C) point to an increase in seismic airgun activity above 30 Hz in 2012, compared to 2005.

Near Wake Island, the difference matrices for both the north and south receivers, Figs. 5(E) and 5(F), show a substantial change in the 20–30 Hz range. Compared to the first full year of analysis, from May 2007 to April 2008, contributions to the sound field from biologics in the 20–30 Hz band became more prevalent in 2012. This change in the 20–30 Hz sound field is reflected in the circled regions of the spectrogram in Figs. 6(E) and 6(F). An example of the fin whale vocalizations dominating the 10–30 Hz band at the end of 2007 is shown in inset (iii) of Fig. 6(F). In 2007, the fin whale call structure did not extend higher than approximately 20 Hz. In 2012, a different call structure is displayed in Fig. 6(F) inset (iv). A 10–30 Hz pulse was added to the fin whale song. Though the spectrograms in Figs. 6(E) and 6(F)

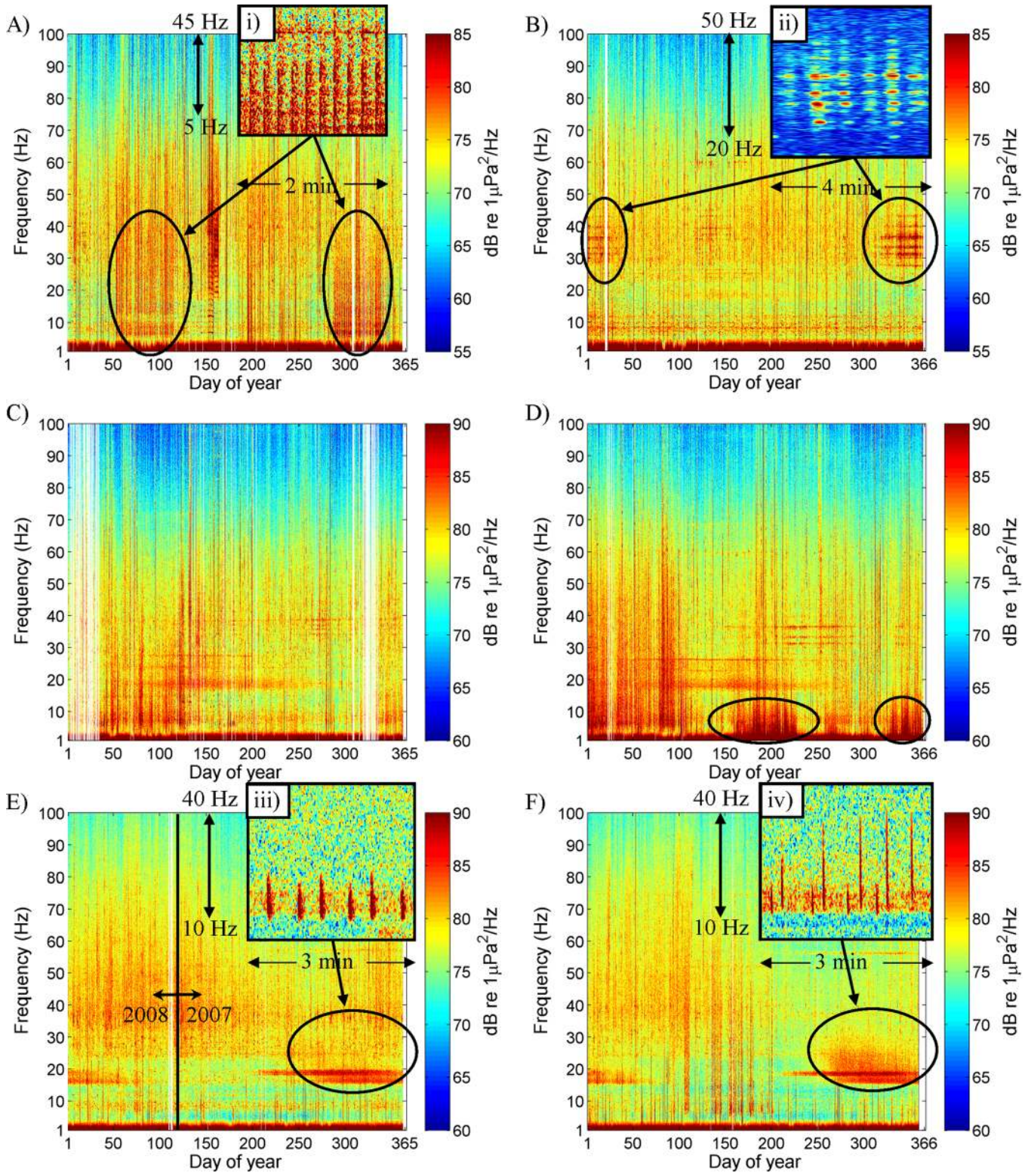

FIG. 6. (Color online) Year-long spectrograms of the sound field at: Diego Garcia North (N1) in (A) 2003 and (B) 2012, Diego Garcia South (S2) in (C) 2003 and (D) 2012, and Wake Island South (S1) from (E) May 2007 to April 2008 and (F) 2012. Circles highlight specific features discussed in the text.

only show the south side of Wake Island, a very similar change occurred on the north side of the island.

IV. DISCUSSION

Low frequency ocean sound trends observed in the South Atlantic Ocean at Ascension Island and Equatorial Pacific at Wake Island do not support a conclusion that ocean sound levels are uniformly increasing across the globe. This work corroborates and extends the frequency range of Matsumoto *et al.* (2014) that reported a decreasing trend observed in very narrow frequency bands (10–13 and 30–36 Hz) in relation to Antarctic ice dynamics. The ambient sound floor in this study showed a decrease in sound

level over the past 5–8 yr across all frequency bands examined. These trends are in stark contrast to the low frequency increases observed in the Northeast Pacific from the 1960s–mid-1990s and in Indian Ocean over the past decade (Ross, 1993, 2005; Andrew *et al.,* 2002; McDonald *et al.,* 2006; Chapman and Price, 2011; Miksis-Olds *et al.,* 2013, 2014), yet are consistent with the recent decreases in the Northeast Pacific over the same approximate time period (Andrew *et al.,* 2011). Increase in shipping was the primary driver cited in association with the observed increases in the Northeast Pacific and Indian Oceans (Andrew *et al.,* 2002; McDonald *et al.,* 2006; McKenna *et al.,* 2012; Frisk, 2012; Miksis-Olds *et al.,* 2013). Ship movements were acquired from Lloyd's List Intelligence (London, UK) in the Pacific Ocean, and as a whole were not observed to increase greatly over the time period for which the CTBTO IMS data were available at this location from 2007 to 2010 (Fig. 7). Over the same time period, quieting technology for ships has improved (NOAA, 2007) which may have resulted in a net sound floor decrease in an area where shipping has remained relatively constant compared to the regional large shipping increases in the Northeast Pacific and Indian Oceans.

Examination of the trends in the outlying percentiles (P1–P10 and P90–P99), in addition to average conditions (P50), is valuable because it provides information on the dynamics of isolated components of the soundscape that are either devoid of identifiable sources (i.e., sound floor) or driven by the loudest sources attributable to specific source categories (i.e., natural seismic events, regional seismic airgun activity) The observed decrease in the sound floor and lower percentiles is noteworthy because it reflects the trend during the quietest periods of time when no transient sound sources are present, and contributions to the soundscape is energy from perpetual wave–wind dynamics, long distance shipping, and turbulent pressure fluctuations. It is this baseline component of the soundscape that will be of interest in future studies related to the ubiquitous effects of ocean acidification and its potential impact on ocean noise via changes in the acoustic absorption coefficient at low frequencies (Hester *et al.,* 2008; Reeder and Chiu, 2010; Browning *et al.,* 2014). Likewise, understanding trends in the loudest source mechanisms is valuable to studies of masking and noise compensation related to marine mammal behavior and vocal activity (Miller *et al.,* 2008; Parks *et al.,* 2011; Hotchkin and Parks, 2013). The most extreme percentiles may also prove useful in tracking climate change through the occurrence of high intensity storms, as the rate of intense storms is projected to increase due to climate change (Michener *et al.,* 1997).

The use of frequency correlation difference matrices was used to identify changes in source contributions over time in an effort to explain the observed trends. Our ability to fully interpret the information and differences in frequency correlation matrices is still in its infancy, so we have confined our discussion points to the areas indicating the greatest amount of change between a year at the start and end of the data time series. The detailed information available in frequency correlation matrices continue to be explored in on-going work by S. Nichols. Salient aspects of the frequency correlation difference matrices from Ascension Island South and Diego Garcia North reveal a potential relationship between seismic airgun and vocalizing whale detections. At Ascension South, there were no significant increases observed for any percentile or frequency band, and the interpretation of the highest areas of correlation coefficient differences at this location suggests a change in the dominant source from seismic airgun signals in 2005 to vocalizing baleen whales in 2012. At Diego Garcia North, the ambient sound floor increased over the past decade (Miksis-Olds *et al.,* 2013), and the frequency correlation difference matrix identified that the greatest areas of change between 2003 and 2012 occurred in the 5–20 and 30–40 Hz bands. Combining the information from the frequency correlation difference matrix with the yearlong spectrograms, seismic airgun activity contributed less to the soundscape in 2012 compared to 2003, and blue whale vocalizations contributed more to the soundscape in 2012 than in 2003. At both locations, whale vocalizations increased over the same

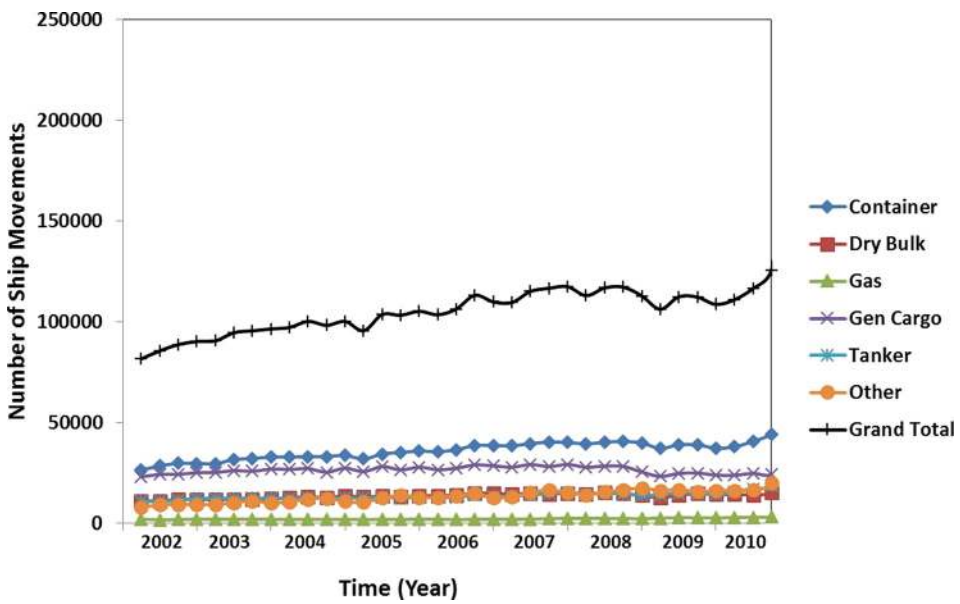

FIG. 7. (Color online) Number of quarterly ship movements in the Equatorial Pacific Ocean basin from Q1 2002 through Q4 of 2010. Data were acquired from Lloyd's List Intelligence. No weighting by vessel class was applied when determining the grand total of vessel movements, so individual time series were also included for each vessel class.

time period as seismic airgun activity decreased. This observation does not provide evidence of a cause–effect relationship, as many other factors, such as ice dynamics (Matsumoto *et al.*, 2014), contribute to the changing soundscapes and to patterns of vocal activity. However, it does raise the question as to whether whales detect and respond to seismic activity originating from hundreds of kilometers away. Low frequency sound in the vicinity of the CTBTO IMS sensors can propagate over the same spatial scales (~1000 km) as whales migrate over (Miksis-Olds *et al.*, 2015). Whether or not, or under what circumstances, long distance seismic activity influences whale migration is unknown, as this trend was not observed to the south of Ascension Island where sound levels were generally higher compared to the northern recordings.

At Ascension North, the salient feature emerging from the difference correlation matrices was a source shift in frequencies above 30 Hz, which was linked to increased seismic airgun activity in 2012 compared to 2005. Seismic airgun pulses have concentrated energy over a broad range of frequencies ranging from <10 Hz to over 70 Hz (Webb, 1998; Tolstoy *et al.*, 2004) [Fig. 5(C)]. This is the likely driver of an increasing sound level trend in the higher (P90 and P99) percentiles at this location in the 40–60 Hz frequency band and also reflected in the full spectrum. At the same time and over the same frequency band, the ambient sound floor and P10 percentile showed a decreasing trend, and the median sound level parameter showed no significant change over the 8 yrs observed. This clearly illustrates the utility and importance of examining multiple sound level parameters in assessing trends and ambient sound dynamics over time. If only the median levels had been analyzed, the decreases in the sound floor and increases in the contribution of the loudest sound sources would have been overlooked; subsequently, the source change identified through the frequency correlation matrices could have been misinterpreted.

The full spectrum and frequency band trends, as well as the difference correlation matrices, were almost identical in the north and south recordings at Wake Island. The uniformity in the sound field indicates that the source mechanisms contributing to the soundscape around Wake Island have been similar since 2007. Decreases were observed in all percentiles from 2007 to 2012, with the exception of an increase in the highest percentile in the 10–30 Hz band that was also reflected in the P99 trend of the full spectrum. The combined information of the spectrograms and frequency correlation matrices suggest that the increasing trend in the 10–30 Hz band was due to a change in structure of fin whale vocalizations.

Although this work showed a recent decreasing trend in specific components of low frequency sound levels at Wake Island, it is likely that there has been an overall increase compared to the early 1980s (McCreery *et al.*, 1993) (Fig. 8). The data from this study are not directly comparable to the McCreery *et al.* (1993) analysis because the previous study removed loud transient signals (earthquakes, close ships, seismic airgun activity) with a power level at least 3 dB greater than the level of the two adjacent samples in the time series, whereas the spectra presented in Fig. 8 include all transients.

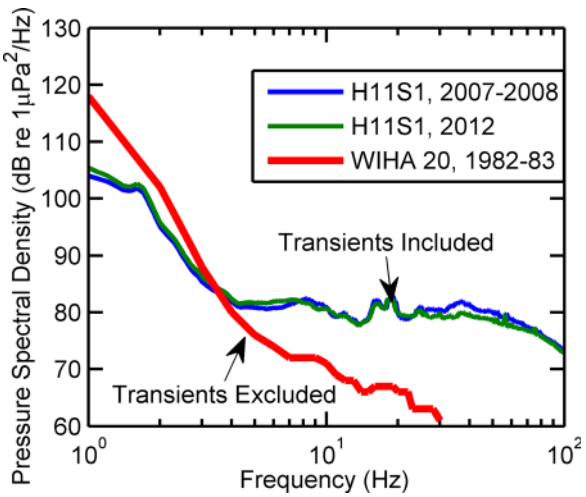

FIG. 8. (Color online) Geometric mean spectra from H11 Wake Island South (S1), representing May 2008 through April 2009 and the full year of 2012. Also included is the average spectrum of a year of measurements from September 1982 to September 1983 at the Wake Island Hydrophone Array (WIHA) hydrophone 20, sampled to exclude transient events (McCreery *et al.*, 1993).

In the wind dominated, lower frequency region (<5 Hz) there is less difference compared to frequencies greater than 5 Hz which exceed the Wenz curve extremes related to heavy shipping traffic (Wenz, 1962), indicating that anthropogenic contributions due to shipping, seismic airgun activity, etc., have increased over time. Assuming an overall increase in sound levels followed by a more recent decrease or no trend, the trends observed at Wake Island in the Equatorial Pacific mimic the multi-decadal patterns observed in the Northeast Pacific (Andrew *et al.*, 2011) and support the theory by Ross (1993) that the 3 dB/decade rate of increase observed in the Northeast Pacific prior to 1980 would not be sustained long term.

V. CONCLUSION

This study adds to the growing body of literature describing long term trends in ocean sound levels. The initial observation of a 3 dB per decade increase in low frequency sound levels in the Northeast Pacific was of grave concern and sparked efforts to determine whether this was a global and continuing phenomenon. Analyses of data from the past decade at CTBTO IMS locations Ascension Island and Wake Island showed decreases in the ambient sound floor, as well as decreases in other sound level parameters. The combination of information harvested from both long term spectrograms and frequency correlation matrices provided insight into the likely sources driving the observed trends, and is a useful method for identifying major source changes contributing to the soundscape over time.

ACKNOWLEDGMENTS

Thanks are extended to James Neely (AFTAC), Richard Baumstark (AFTAC), Mark Prior (CTBTO), and Andrew Forbes (CTBTO) for their assistance in data transfer and transfer of knowledge of CTBTO data. Gratitude is also extended to Chad Smith and Russell Hawkins at ARL Penn

State for their assistance in data processing and figure contributions. David L. Bradley provided comments on an earlier draft of this manuscript, and his comments are greatly appreciated. This work was supported by an Office of Naval Research (ONR) Young Investigator Program Award (N000141110619) to J.L.M.O. and ONR Ocean Acoustics Award (N000141110039) to David L. Bradley.

Andrew, R. K., Howe, B. M., and Mercer, J. A. (**2011**). "Long-time trends in ship traffic noise for four sites off the North American West Coast," J. Acoust. Soc. Am. **129**, 642–651.

Andrew, R. K., Howe, B. M., Mercer, J. A., and Dzieciuch, M. A. (**2002**). "Ocean ambient sounds: Comparing the 1960's with the 1990's for a receiver off the California coast," ARLO **3**, 65–70.

Browning, D., Herstein, P. D., Scheifele, P. M., and Hasse, R. W. (**2014**). "Low frequency sound absorption in the Arctic Ocean: Potential impact of ocean acidification," J. Acoust. Soc. Am. **135**, 2306.

Chapman, N. R., and Price, A. (**2011**). "Low frequency deep ocean ambient noise trend in the Northeast Pacific Ocean," J. Acoust. Soc. Am. **129**, EL161–EL165.

Frisk, G. V. (**2012**). "Noiseonomics: The relationship between ambient noise levels and global economic trends," Sci. Rep. **2**, 437.

Gavrilov, A., and Li, B. (**2008**). "Long-term variations of ice breaking noise in Antarctica," J. Acoust. Soc. Am. **123**, 2989–2990.

Gavrilov, A. N., McCauley, R. D., and Gedamke, J. (**2012**). "Steady inter and intra-annual decreases in the vocalization frequency of Antarctic blue whales," J. Acoust. Soc. Am. **131**, 4476–4480.

Hester, K. C., Peltzer, E. T., Kirkwood, W. J., and Brewer, P. G. (**2008**). "Unanticipated consequences of ocean acidification: A noisier ocean at lower pH," Geophys. Res. Lett. **35**, L19601, doi:10.1029/2008GL034913.

Hotchkin, C., and Parks, S. (**2013**). "The Lombard effect and other noise-induced vocal modifications: Insight from mammalian communication systems," Biol. Rev. **88**, 809–824.

Klinck, H., Nieukirk, S. L., Mellinger, D. K., Klinck, K., Matsumoto, H., and Dziak, R. P. (**2012**). "Seasonal presence of cetaceans and ambient noise levels in polar waters of the North Atlantic," J. Acoust. Soc. Am. Exp. Lett. **132**, EL176–EL181.

Matsumoto, H., Bohnenshiehl, D. R., Tournadre, J., Dziak, R. P., Haxel, J. H., Lau, T. K. A., Fowler, M., and Sigrid, S. (**2014**). "Antarctic icebergs: A significant natural ocean sound source in the Southern Hemisphere," Geochem. Geophys. Geosyst. **15**, 3448–3458, doi:10.1002/2014GC005454.

McCreery, C. S., Duennebier, F. K., and Sutton, G. H. (**1993**). "Correlation of deep ocean noise (0.4–30Hz) with wind, and the Holu Spectrum-A worldwide constant," J. Acoust. Soc. Am. **93**, 2639–2648.

McDonald, M. A., Hildebrand, J. A., and Mesnick, S. (**2009**). "Worldwide decline in tonal frequencies of blue whale songs," Endangered Species Res. **9**, 13–21.

McDonald, M. A., Hildebrand, J. A., and Wiggins, S. M. (**2006**). "Increases in deep ocean ambient noise in the Northwest Pacific west of San Nicolas Island, California," J. Acoust. Soc. Am. **120**, 711–717.

McKenna, M. F., Katz, S. L., Wiggins, S. M., Ross, D., and Hildebrand, J. A. (**2012**). "A quieting ocean: Unintended consequence of a fluctuating economy," J. Acoust. Soc. Am. **132**, EL169–EL175.

Michener, W. K., Blood, E. R., Bildstein, K. L., Brinson, M. M., and Gardner, L. R. (**1997**). "Climate change, hurricanes and tropical storms, and rising sea level in coastal wetlands," Ecol. Appl. **7**, 770–801.

Miksis-Olds, J. L., Bradley, D. L., and Niu, X. M. (**2013**). "Decadal trends in Indian Ocean ambient sound," J. Acoust. Soc. Am. **134**, 3464–3475.

Miksis-Olds, J. L., Bradley, D. L., and Niu, X. M. (**2014**). "Erratum: Decadal trends in Indian Ocean ambient sound [J. Acoust. Soc. Am. **134**(5), 3464–3475 (2013)]," J. Acoust. Soc. Am. **135**, 1642.

Miksis-Olds, J. L., Vernon, J. A., and Heaney, K. D. (**2015**). "The impact of ocean sound dynamics on estimates of signal detection range," Aquat. Mamm. **41**(4), 444–454.

Miller, J. H., Nystuen, J. A., and Bradley, D. L. (**2008**). "Ocean noise budgets," Bioacoustics **17**, 133–136.

Nieurkirk, S. L., Mellinger, D. K., Moore, S. E., Klinck, K., Dziak, R. P., and Goslin, J. (**2012**). "Sounds from airguns and fin whales recorded in the mid-Atlantic Ocean, 1999−2009," J. Acoust. Soc. Am. **131**, 1102–1112.

NOAA (National Oceanic and Atmospheric Administration) (**2007**). "International symposium 'Potential application of vessel quieting technology on large commercial vessels'," NOAA Ocean Acoustics Program. http://www.nmfs.noaa.gov/pr/pdfs/acoustics/vessel_symposium_report.pdf (Last viewed 11/18/15).

Parks, S. E., Johnson, M., Nowacek, D., and Tyack, P. L. (**2011**). "Individual right whales call louder in increased environmental noise," Biol. Lett. **7**, 33–35.

Pulli, J. J., and Upton, Z. M. (**2001**). "Hydroacoustic blockage at Diego Garcia: Models and observations," *23rd Seismic Research Review: Worldwide Monitoring of Nuclear Explosions*. October 2–5, 2001, Vol. 2, pp. 45–54.

Reeder, D. B., and Chiu, C. S. (**2010**). "Ocean acidification and its impacts on ocean noise: Phenomenology and analysis," J. Acoust. Soc. Am. **128**, EL137–EL143.

Ross, D. (**1993**). "On ocean underwater ambient noise," Acoust. Bull. **18**, 5–8.

Ross, D. (**2005**). "Ship sources of ambient noise," IEEE J. Ocean. Eng. **30**, 257–261.

Samaran, F., Adam, O., and Guinet, C. (**2010**). "Detection range modeling of blue whale calls in the Southwestern Indian Ocean," Appl. Acoust. **71**, 1099–1106.

Stafford, K. M., Bohnenstiehl, D. R., Tolstoy, M., Chapp, E., Mellinger, D. K., and Moore, S. E. (**2004**). "Antarctic-type blue whale calls recorded at low latitudes in the Indian and eastern Pacific Oceans," Deep Sea Res., Part I **51**, 1337–1346.

Tolstoy, M., Diebold, J. B., Webb, S. C., Bohnenstiehl, D. R., Chapp, E., Holmes, R. C., and Rawson, M. (**2004**). "Broadband calibration of R/V Ewing seismic sources," Geophys. Res. Lett. **31**, L14310, doi:10.1029/2004GL020234.

Webb, S. C. (**1998**). "Broadband seismology and noise under the ocean," Rev. Geophys. **36**, 105–142, doi:10.1029/97RG02287.

Wenz, G. M. (**1962**). "Acoustic ambient noise in the ocean: Spectra and sources," J. Acoust. Soc. Am. **34**, 1963–1956.

Wilcock, W. S. D., Stafford, K. M., Andrew, R. K., and Odom, R. I. (**2014**). "Sounds in the ocean at 1–100 Hz," Ann. Rev. Mar. Sci. **6**, 117–140.